Quantum Electronics **46** (9) 848–854 (2016)

NANOFOCUSING DOI: 10.1070/QEL16065

Focusing of light at the nanoapex of a metal microtip located above the plane of a dielectric or metal

A.B. Petrin

Abstract. **We study the focusing of the optical electromagnetic radiation energy into a nanoscale spatial region in the vicinity of the nanoapex of a metal microtip located near a dielectric or metal plane. Focusing arises from a symmetric convergence of a surface plasmon TM wave at the nanoapex. The metal boundary near the nanoapex is approximated by a paraboloid of revolution. A numerical model, based on the method of moments, is developed to find the electric field near the tip apex. Calculation results show that, compared to a single tip, the presence of a plane leads to an additional concentration of the electric field near the nanoapex.**

Keywords: *nanofocusing, surface plasmons, plasmon waveguide.*

1. Introduction

Nanofocusing of light energy at the apex of a microtip is the most important phenomenon that underlies the promising nanotechnology applications. One of the manifestations of nanofocusing is an unusually sharp increase in the intensity of a surface plasmon polariton, symmetrically excited at the base of a conical metal microtip, when it symmetrically converges at the nanoapex [1–3]. This phenomenon is explained by the fact that on a geometrically perfect metal tip, there can exist an axially symmetric electromagnetic standing wave with a singularity of the electric field at the apex [4, 5]. Experiments have shown [6, 7] that this wave can be efficiently excited by a convergent surface plasmon TM wave with the same axial field symmetry. The presence of the singularity of the electric field is well explained in the quasi-static approximation, which is fulfilled in the vicinity of the nanoapex of a metal microtip.

A real apex of a microtip is not ideal and has a rounding. In papers [8, 9], to find the electric field distribution on a rounded top of a single microtip, the surface of the apex was approximated by a paraboloid of revolution and the problem was solved in the paraboloidal coordinate system. It has been shown that the characteristic size of the focal distribution at the tip apex decreases in proportion to its radius of curvature, which explains nanofocusing.

In this paper we study how the focal field distribution changes if the apex of the tip is located near the flat surface of a material (for example, by scanning the surface with the tip).

A.B. Petrin Joint Institute for High Temperatures, Russian Academy of Sciences, ul. Izhorskaya 13, Bld. 2, 125412 Moscow, Russia; e-mail: a_petrin@mail.ru

Received 14 March 2016; revision received 9 July 2016
Kvantovaya Elektronika **46** (9) 848–854 (2016)
Translated by I.A. Ulitkin

It should be noted that an increase in the electromagnetic optical field on sharp edges and tips has already been considered in relation to other problems [10–12]. In addition, attempts to solve the problem of finding a field at the top of a tip near a flat structure have already been made in [13]. However, for simplification Passian et al. [13] considered the problem in which the tip has the form of a hyperboloid of revolution, which is located above the half-space whose boundary corresponds to the coordinate surface of a spherical coordinate system. In this formulation of the problem with a fixed geometry of the tip (for fixed values of the focal length of the hyperboloid and the apex radius), it is impossible to change independently the distance to the plane boundary (this distance is uniquely determined by the geometry of the tip).

The method used in this paper, as will be shown below, is free from this drawback.

2. Electric field distribution at the nanoapex of a metal microtip located near a plane boundary in the quasi-static approximation. Formulation of the problem

Consider a metal microtip with a nanoscale radius of curvature R. Let the surface of the tip near the apex be described by the paraboloid of revolution $z = R/2 - (x^2 + y^2)/(2R)$ (axially symmetric with respect to the z axis) (Fig. 1). Suppose also that near the tip there is a perpendicular plane defined by the

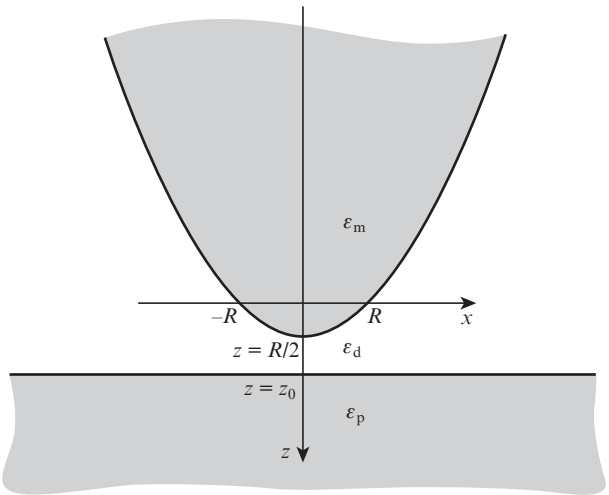

Figure 1. Geometry of the problem.

equation $z = z_p$, where $z_p \geqslant R/2$. The complex dielectric constants of the metal tip, external homogeneous medium and semi-infinite medium at $z \geqslant z_p$ are denoted by ε_m, ε_d and ε_p, respectively.

In solving the problem we will use a complex representation of the fields with a temporal dependence of form $\exp(-i\omega t)$, where ω is the cyclic frequency. The problem can be solved in the quasi-static approximation [8], in which the potential of the electric field Φ obeys the Laplace equation $\Delta\Phi = 0$, and the normal and tangential components of the electric field on the surface of the tip and the plane should meet the known boundary conditions, namely:

$$\varepsilon_d E_{dn} = \varepsilon_m E_{mn} \text{ and } E_{d\tau} = E_{m\tau} \tag{1a}$$

on the surface of the tip and

$$\varepsilon_p E_{pn} = \varepsilon_d E_{dn} \text{ and } E_{p\tau} = E_{d\tau} \tag{1b}$$

on the plane.

We seek an axisymmetric solution to the Laplace equation, which has a maximum of the field at the tip apex and corresponds to the focusing of a TM-mode surface plasmon wave at the microtip.

In addition, to automatically satisfy the boundary conditions on the plane (1b), we will use the method of mirror images. Its essence, as applied to the problem under study, is as follows: let the potential of charges on a paraboloidal metal tip in space with a dielectric constant ε_d be described by the function $\Phi_{tip}(\boldsymbol{r}) = \Phi_{tip}(x,y,z)$, where the radius vector $\boldsymbol{r} = (x,y,z)$ passes through the origin of the coordinates to the point of determining the potential. In this case, the expression for the potential of induced charges on a plane boundary of dielectrics in space with the dielectric constant ε_d can be written in the form [14]

$$\Phi_{ref}(\boldsymbol{r}) = -\frac{\varepsilon_p - \varepsilon_d}{\varepsilon_p + \varepsilon_d}\Phi_{tip}(\boldsymbol{r}_{ref}),$$

where $\boldsymbol{r}_{ref} = (x,y,2z_0 - z)$. Then, in a region filled with a dielectric having a dielectric constant ε_d, the total potential is

$$\Phi_d(\boldsymbol{r}) = \Phi_{tip}(\boldsymbol{r}) + \Phi_{ref}(\boldsymbol{r}) = \Phi_{tip}(x,y,z) - \frac{\varepsilon_p - \varepsilon_d}{\varepsilon_p + \varepsilon_d}\Phi_{tip}(x,y,2z_0 - z). \tag{2}$$

The potential of all the tip charges and the charges induced on a plane boundary (it follows from Maxwell's equations that inside a homogeneous dielectric, the polarisation charges are absent because they can only be at the boundary) in half-space filled with a dielectric having a dielectric constant ε_p can be written in the form

$$\Phi_p(\boldsymbol{r}) = \frac{2\varepsilon_d}{\varepsilon_p + \varepsilon_d}\Phi_{tip}(\boldsymbol{r}) = \frac{2\varepsilon_d}{\varepsilon_p + \varepsilon_d}\Phi_{tip}(x,y,z). \tag{3}$$

The correctness of formulas (2), (3) follows from the uniqueness theorem and from the automatic fulfillment of conditions (1b) at the boundary of the half-space.

Let us now find a general expression for the potential of tip charges $\Phi_{tip}(\boldsymbol{r})$, satisfying the Laplace equation in a homogeneous dielectric space (without a plane) inside and outside of the tip; in this case, conditions (1a) must be satisfied on the boundary. We introduce paraboloidal coordinates [15] (or a system of parabolic coordinates of revolution) α,β,ψ, which are related to rectangular Cartesian coordinates x,y,z by the expressions

$$x = c\alpha\beta\cos\psi,\ y = c\alpha\beta\sin\psi,\ z = \frac{1}{2}c(\beta^2 - \alpha^2), \tag{4}$$

where c is a constant scaling factor. In the coordinate system in question (Fig. 1), the Laplace equation for the electric potential Φ inside and outside of the tip under conditions of the axial symmetry (Φ does not depend on ψ) can be written in the form [15]:

$$\Delta\Phi = \frac{1}{c^2(\alpha^2 + \beta^2)}\left(\frac{\partial^2\Phi}{\partial\alpha^2} + \frac{\partial^2\Phi}{\partial\beta^2} + \frac{1}{\alpha}\frac{\partial\Phi}{\partial\alpha} + \frac{1}{\beta}\frac{\partial\Phi}{\partial\beta}\right) = 0. \tag{5}$$

The general solution of (5) is known [15] and is given by

$$\Phi = \sum[B_1 J_0(p\alpha) + B_2 Y_0(p\alpha)][C_1 I_0(p\beta) + C_2 K_0(p\beta)], \tag{6}$$

where p, B_1, B_2, C_1, C_2 are the constants; J_0 and Y_0 are the zero-order Bessel functions of the first and the second kind; and I_0 and K_0 are the modified zero-order Bessel functions of the first and the second kind. The summation is performed over all solutions with different values of the constants.

Let the boundary of a paraboloidal tip be determined by the equation $\beta = \beta_0$. It follows from (4) that the tip boundary $\beta = \beta_0$ in the Cartesian coordinates x,y,z is described by the equation $z = c\beta_0^2/2 - (x^2 + y^2)/(2c\beta_0^2)$. It is easy to show that the radius of curvature of the tip apex is $R = c\beta_0^2$.

In what follows we will use the axially symmetric solutions of the Laplace equation. Therefore, to meet the boundary conditions on the entire surface of the rotation of the tip, it is sufficient to satisfy them on the line of intersection of the boundary surface of the tip with any symmetry plane passing through the z axis. As such a plane we choose the plane xz. It is easy to show that in our case it is sufficient to fulfill the boundary conditions only at the boundary of intersection of the half-plane $y = 0$ for $x \geqslant 0$ and the surface of the paraboloidal tip.

For generality of further discussion, we pass in the plane xz to dimensionless coordinates $\tilde{x} = x/R$, $\tilde{z} = z/R$ and $\tilde{\alpha} = \alpha/\beta_0$, $\tilde{\beta} = \beta/\beta_0$. Dimensionless paraboloidal $(\tilde{\alpha},\tilde{\beta})$ and Cartesian $(\tilde{x},\tilde{z})$ coordinates on the plane $\tilde{x}\tilde{z}$ are related by the expressions

$$\tilde{\alpha} = (\sqrt{\tilde{x}^2 + \tilde{z}^2} - \tilde{z})^{1/2} \text{ and } \tilde{\beta} = \tilde{x}(\sqrt{\tilde{x}^2 + \tilde{z}^2} - \tilde{z})^{-1/2}$$

at positive $\tilde{x}$ [8]. In these coordinates, the tip boundary is given by the expression $\tilde{z} = 1/2 - \tilde{x}^2/2$, and the Laplace equation (5) in the dimensionless coordinates has the form

$$\frac{1}{(\tilde{\alpha}^2 + \tilde{\beta}^2)}\left(\frac{\partial^2\Phi}{\partial\tilde{\alpha}^2} + \frac{\partial^2\Phi}{\partial\tilde{\beta}^2} + \frac{1}{\tilde{\alpha}}\frac{\partial\Phi}{\partial\tilde{\alpha}} + \frac{1}{\tilde{\beta}}\frac{\partial\Phi}{\partial\tilde{\beta}}\right) = 0.$$

If the axially symmetric potential is found from the solution of the Laplace equation, i.e. if it is a function of only $\tilde{\alpha}$ and $\tilde{\beta}$, then the expression for the tangential and normal dimensional components of the field on both sides of the dielectric–metal interface can be written as

$$E_{d\tau} = -\frac{1}{R\sqrt{\tilde{\alpha}^2 + \tilde{\beta}^2}}\frac{\partial\Phi_d}{\partial\tilde{\alpha}},\ E_{dn} = -\frac{1}{R\sqrt{\tilde{\alpha}^2 + \tilde{\beta}^2}}\frac{\partial\Phi_d}{\partial\tilde{\beta}},$$

$$E_{m\tau} = -\frac{1}{R\sqrt{\tilde{\alpha}^2+\tilde{\beta}^2}}\frac{\partial \Phi_m}{\partial \tilde{\alpha}},\ E_{mn} = -\frac{1}{R\sqrt{\tilde{\alpha}^2+\tilde{\beta}^2}}\frac{\partial \Phi_m}{\partial \tilde{\beta}}.$$

We normalise the potential to its U value in the maximum of the field at the tip apex, then we can pass from the dimensional potential to the dimensionless potential $\tilde{\Phi} = \Phi/U$ or from the dimensional field components to their dimensionless quantities:

$$\tilde{E}_{d\tau} = \frac{R}{U}E_{d\tau} = -\frac{1}{\sqrt{\tilde{\alpha}^2+\tilde{\beta}^2}}\frac{\partial \tilde{\Phi}_d}{\partial \tilde{\alpha}},$$

$$\tilde{E}_{dn} = \frac{R}{U}E_{dn} = -\frac{1}{\sqrt{\tilde{\alpha}^2+\tilde{\beta}^2}}\frac{\partial \tilde{\Phi}_d}{\partial \tilde{\beta}},$$

$$\tilde{E}_{m\tau} = \frac{R}{U}E_{m\tau} = -\frac{1}{\sqrt{\tilde{\alpha}^2+\tilde{\beta}^2}}\frac{\partial \tilde{\Phi}_m}{\partial \tilde{\alpha}},$$

$$\tilde{E}_{mn} = \frac{R}{U}E_{mn} = -\frac{1}{\sqrt{\tilde{\alpha}^2+\tilde{\beta}^2}}\frac{\partial \tilde{\Phi}_m}{\partial \tilde{\beta}}.$$

In the normalised Cartesian coordinates, in the plane $\tilde{x}\tilde{z}$ the components of the normalised electric field have the form $\tilde{E}_{\tilde{x}} = -\partial\tilde{\Phi}/\partial\tilde{x}$, $\tilde{E}_{\tilde{z}} = -\partial\tilde{\Phi}/\partial\tilde{z}$. Below, it will be convenient to consider the potential $\tilde{\Phi}_{tip}$ and its gradient as a function of $\tilde{\alpha},\tilde{\beta}$, and $\tilde{\Phi}_{ref}$ and its gradient – as a function of $\tilde{x}$ и $\tilde{z}$ in the $\tilde{x}\tilde{z}$ plane.

Thus, based on the general solution of (6), we seek a solution of the boundary problem for the electric field in the vicinity of the tip, suggesting that the expressions for the potentials $\tilde{\Phi}_{tip}$ outside ($\beta \geqslant \beta_0$) and inside ($\beta \leqslant \beta_0$) of the metal tip have the form

$$\begin{aligned}\tilde{\Phi}_{tip\,d} &= \sum_{j=1}^{N} A_j J_0(q_j\tilde{\alpha})K_0(q_j\tilde{\beta}),\\ \tilde{\Phi}_{tip\,m} &= \sum_{j=1}^{N} B_j J_0(q_j\tilde{\alpha})I_0(q_j\tilde{\beta}),\end{aligned} \tag{7}$$

where A_j, B_j and q_j are the constants. The quantities q_j were chosen in the form $q_j = \mu_j/L$, where μ_j are the first N roots of the Bessel equation $J_0(\mu_j) = 0$, and L is a dimensionless distance from the apex, at which the boundary conditions on the tip surface must be satisfied. In the limit $N \to \infty$, the system of functions $J_0(q_j\tilde{\alpha})$ with the given q_j on the interval $0 \leqslant \tilde{\alpha} \leqslant L$ is a complete system of functions [16].

Note that the choice of functional dependences (7) from the general solution (6) is due to the natural requirements to the field focused at the microtip (which uniquely identify these dependences):

1) outside of the tip the potential should decrease with increasing distance from its surface, be finite and maximal at the top of the tip;

2) inside of the metal tip the potential should be finite at the origin of the coordinates.

In addition, the electric potential should be continuous across the interface.

Substituting (7) into (2), we obtain the potential in the dielectric in the plane $\tilde{x}\tilde{z}$

$$\begin{aligned}\tilde{\Phi}_d(\tilde{x},\tilde{z}) = \sum_{j=1}^{N} A_j J_0\left(q_j\left(\sqrt{\tilde{x}^2+\tilde{z}^2}-\tilde{z}\right)^{1/2}\right)\times\\ \times K_0\left(q_j\tilde{x}\left(\sqrt{\tilde{x}^2+\tilde{z}^2}-\tilde{z}\right)^{-1/2}\right)\\ -\frac{\varepsilon_p-\varepsilon_d}{\varepsilon_p+\varepsilon_d}\sum_{j=1}^{N} A_j J_0\left(q_j\left[\sqrt{\tilde{x}^2+(2\tilde{z}_0-\tilde{z})^2}-(2\tilde{z}_0-\tilde{z})\right]^{1/2}\right)\\ \times K_0\left(q_j\tilde{x}\left[\sqrt{\tilde{x}^2+(2\tilde{z}_0-\tilde{z})^2}-(2\tilde{z}_0-\tilde{z})\right]^{-1/2}\right),\end{aligned} \tag{8}$$

where $\tilde{z}_0 = z_0/R$ is the normalised coordinate of a plane boundary. Similarly, the potential in the metal tip in the plane $\tilde{x}\tilde{z}$ can be written as

$$\begin{aligned}\tilde{\Phi}_m(\tilde{x},\tilde{z}) = \sum_{j=1}^{N} B_j J_0\left(q_j\left(\sqrt{\tilde{x}^2+\tilde{z}^2}-\tilde{z}\right)^{1/2}\right)\\ \times I_0\left(q_j\tilde{x}\left(\sqrt{\tilde{x}^2+\tilde{z}^2}-\tilde{z}\right)^{-1/2}\right).\end{aligned} \tag{9}$$

At the tip boundary (at $\tilde{z} = 1/2 - \tilde{x}^2/2$), the unit vectors of normal and tangential components are described by formulas

$$\boldsymbol{n} = \boldsymbol{e}_{\tilde{x}}\left(\frac{\tilde{x}}{\sqrt{1+\tilde{x}^2}}\right) + \boldsymbol{e}_{\tilde{z}}\left(\frac{1}{\sqrt{1+\tilde{x}^2}}\right),$$

$$\boldsymbol{\tau} = \boldsymbol{e}_{\tilde{x}}\left(\frac{1}{\sqrt{1+\tilde{x}^2}}\right) + \boldsymbol{e}_{\tilde{z}}\left(-\frac{\tilde{x}}{\sqrt{1+\tilde{x}^2}}\right).$$

Then, the boundary conditions for the normal and tangential components of the fields on the surface of the tip can be written using $\tilde{E}_{\tilde{x}} = -\partial\tilde{\Phi}/\partial\tilde{x}$ and $\tilde{E}_{\tilde{z}} = -\partial\tilde{\Phi}/\partial\tilde{z}$, respectively, in the form

$$\begin{aligned}-\varepsilon_d\left(\frac{\tilde{x}}{\sqrt{1+\tilde{x}^2}}\frac{\partial\tilde{\Phi}_d}{\partial\tilde{x}}+\frac{1}{\sqrt{1+\tilde{x}^2}}\frac{\partial\tilde{\Phi}_d}{\partial\tilde{z}}\right)\Bigg|_{\tilde{z}=1/2-\tilde{x}^2/2}\\ +\varepsilon_m\left(\frac{\tilde{x}}{\sqrt{1+\tilde{x}^2}}\frac{\partial\tilde{\Phi}_m}{\partial\tilde{x}}+\frac{1}{\sqrt{1+\tilde{x}^2}}\frac{\partial\tilde{\Phi}_m}{\partial\tilde{z}}\right)\Bigg|_{\tilde{z}=1/2-\tilde{x}^2/2}=0,\end{aligned} \tag{10}$$

$$\begin{aligned}-\left(\frac{1}{\sqrt{1+\tilde{x}^2}}\frac{\partial\tilde{\Phi}_d}{\partial\tilde{x}}-\frac{\tilde{x}}{\sqrt{1+\tilde{x}^2}}\frac{\partial\tilde{\Phi}_d}{\partial\tilde{z}}\right)\Bigg|_{\tilde{z}=1/2-\tilde{x}^2/2}\\ +\left(\frac{1}{\sqrt{1+\tilde{x}^2}}\frac{\partial\tilde{\Phi}_m}{\partial\tilde{x}}-\frac{\tilde{x}}{\sqrt{1+\tilde{x}^2}}\frac{\partial\tilde{\Phi}_m}{\partial\tilde{z}}\right)\Bigg|_{\tilde{z}=1/2-\tilde{x}^2/2}=0.\end{aligned} \tag{11}$$

If we substitute expressions (8), (9) into (10), (11), we obtain linear equations for A_j and B_j, which can be expressed as

$$-\varepsilon_d\sum_{j=1}^{N} A_j f_j(q_j,\tilde{x}) + \varepsilon_m\sum_{j=1}^{N} B_j g_j(q_j,\tilde{x}) = 0, \tag{12}$$

$$-\sum_{j=1}^{N} A_j h_j(q_j,\tilde{x}) + \sum_{j=1}^{N} B_j t_j(q_j,\tilde{x}) = 0. \tag{13}$$

For brevity, we will not write here expressions for the functions $f_j(q_j,\tilde{x})$, $g_j(q_j,\tilde{x})$, $h_j(q_j,\tilde{x})$ and $t_j(q_j,\tilde{x})$ in an explicit form, which can be obtained at this trivial substitution.

Equations (12), (13) were solved by the method of moments [17]. Given the fact that on the surface of the tip (at $\tilde{z} = 1/2 - \tilde{x}^2/2$) $\tilde{\alpha} = \tilde{x}$ and $\tilde{\beta} = 1$, as the weight functions on the boundaries at $0 \leqslant \tilde{x} \leqslant L$, we chose the functions $W_i = J_0(q_i\tilde{x})$, which in the interval $0 \leqslant \tilde{x} \leqslant L$ in the limit $N \to \infty$ form a complete system of functions with a scalar product

$$\langle W_i, F_j \rangle = \int_0^L W_i \tilde{x} F_j \mathrm{d}\tilde{x}\,.$$

Then, after multiplying scalarly equations (12) and (13) by W_i ($i = 1, ..., N-1$), we obtained $2N-2$ linear algebraic equations with $2N$ unknowns. To find the unique solution we added another two equations: we equated the potentials outside and inside of the tip to unity. The solution of the resulting system of $2N$ equations determined the potential of the electric field in the entire space, normalised to unity at the top of the tip.

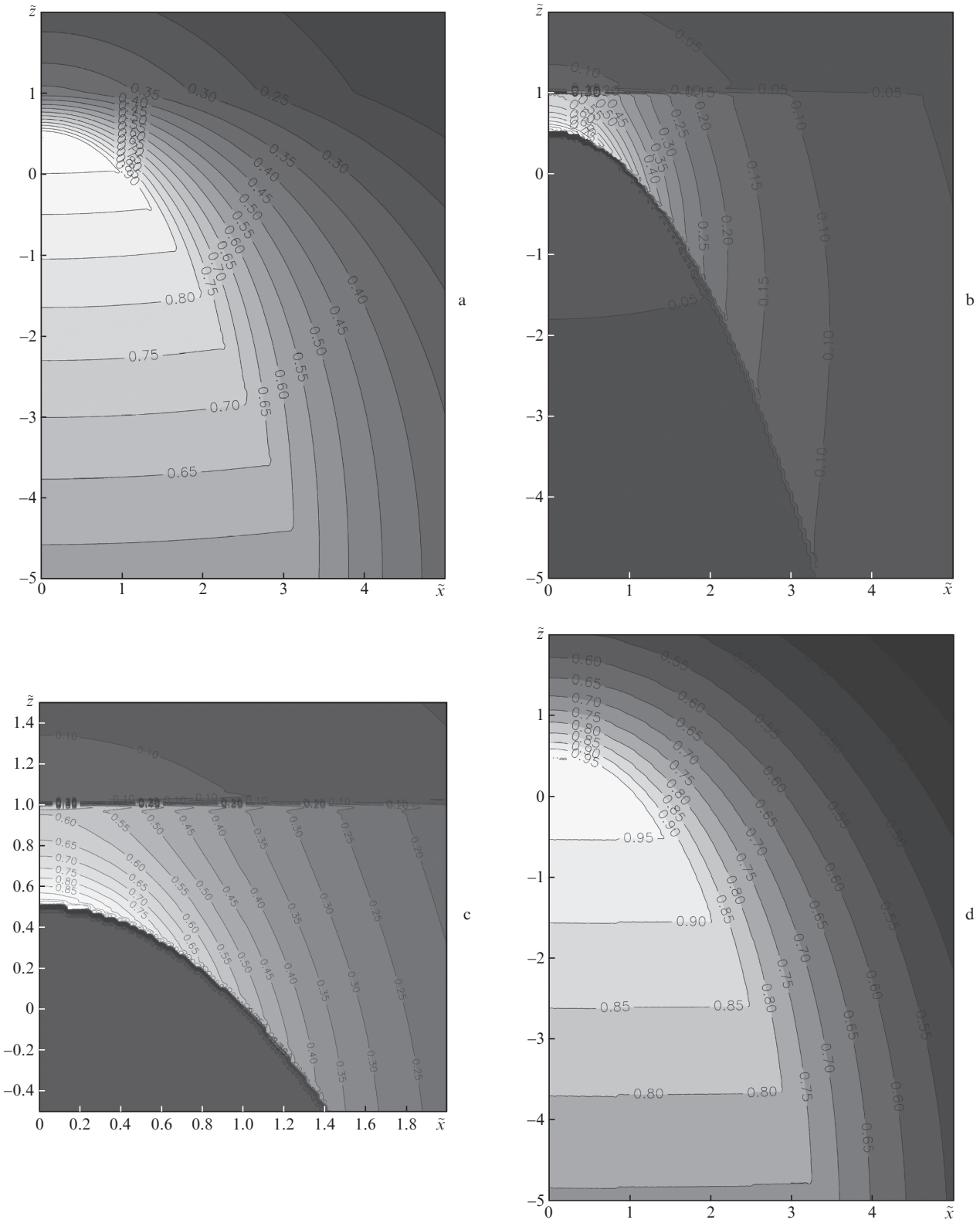

Figure 2. Focal distributions of (a) the electric potential modulus $|\tilde{\Phi}|$ and (b, c) a maximum field E_a for a silver tip near the flat surface $\tilde{z}_0 = 1$ of the half-space with $\varepsilon_p = 4$ at a frequency $\tilde{\omega} = 0.26053$. For comparison, shown is (d) the distribution $|\tilde{\Phi}|$ for a single tip.

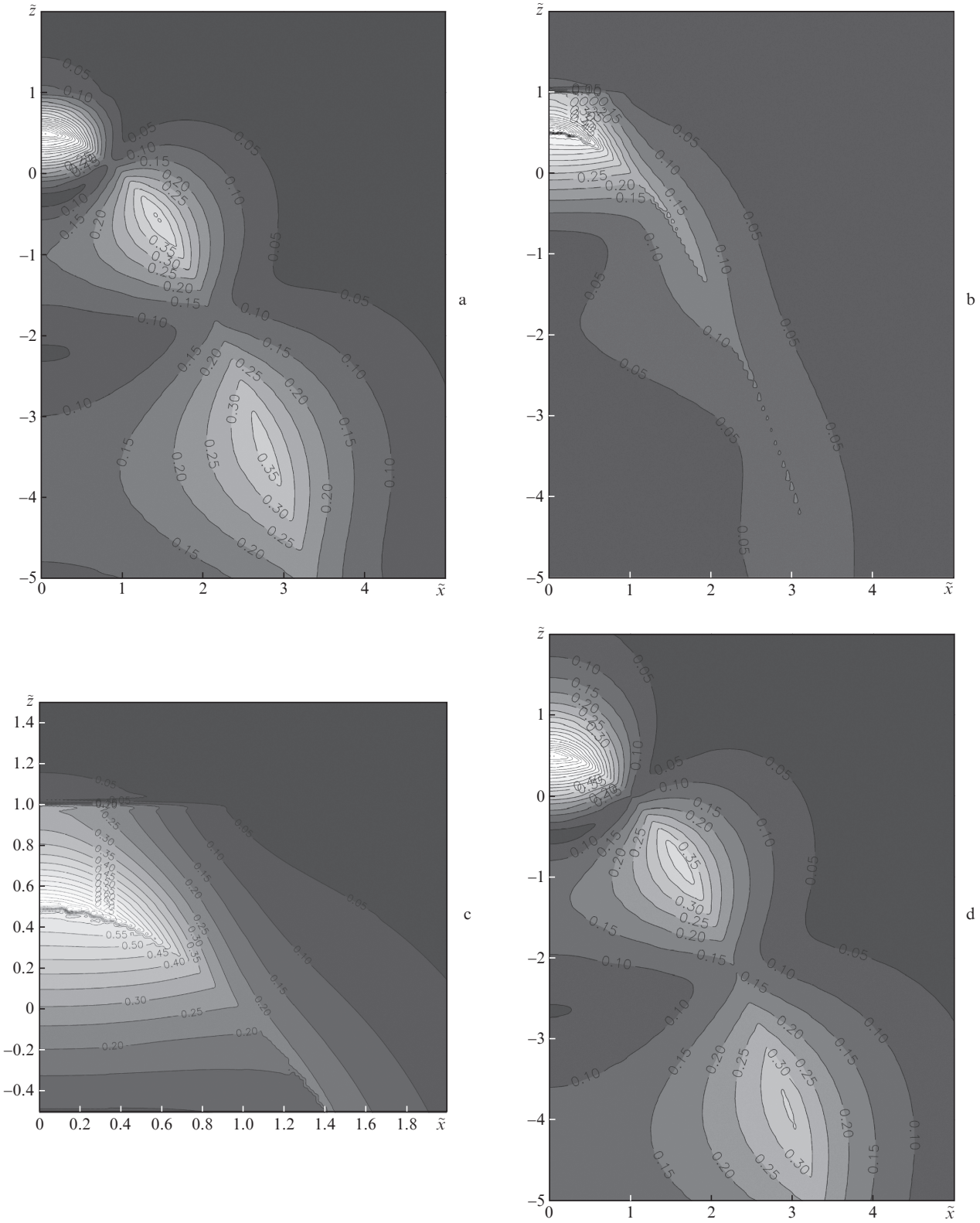

Figure 3. Same as in Fig. 2, but for a frequency $\tilde{\omega} = 0.62252$.

The above choice of the weight functions can satisfy, in the limit $N \to \infty$, the boundary conditions on the surface of the tip at $0 \leqslant \tilde{x} \leqslant L$. The value of L in the calculations was chosen sufficiently large, compared with the size of the domain in which computations of the fields were carried out.

Finally, we should once again discuss the logic of deriving expressions (8), (9) as the only solution in the vicinity of the tip apex and in the gap between the top of the tip and the plane. There are two reasons for an increase in the electric field of the light wave approaching the apex of the tip. The first one

is the convergence of the light wave, excited in the form of a surface plasmon (symmetric with respect to the axis) TM mode [1], at the apex of the tip. Symmetrical convergence of the surface wave leads to the formation of a symmetric field of a standing wave in the vicinity of the tip apex. The second reason is an increase in the field at the top of any tip. In the vicinity of a nanoapex, one can take advantage of the quasi-stationary approximation, requiring that the electric potential satisfies the Laplace equation, the general solution to which is given by formula (6). The mentioned increase in the field and the presence of its maximum at the tip apex uniquely determine from (6) the only kind of the solution for the standing wave (7) with a maximum of the field at the tip apex. In the case of a single tip, the solution is given by an only term with a fixed q. In the presence of a plane boundary in the half-space, we obtain a series with different values of q_j. Note that, as shown in [18], the TE mode cannot exist at the frequencies considered in the paper. The same paper also presents the proof of the applicability of the quasi-stationary approximation.

3. Investigation of focal distributions of the electric potential and the electric field at the nanotip apex near the flat surface of the material

Numerical calculations were carried out for a silver tip near a plane boundary of a dielectric or metal. The dielectric constant of the metal tip is approximately described by the Drude formula $\varepsilon_m = 1 - \omega_p^2/(\omega^2 + i\omega\Gamma)$, where ω_p is the plasma frequency of the metal, and Γ is the coefficient taking into account losses. For silver we used the parameters $\omega_p \approx 1.36\times10^{16}$ s^{-1} and $\Gamma \approx 2\times10^{14}$ s^{-1} [19]. It is convenient to express ε_m through the normalised frequency $\tilde{\omega} = \omega/\omega_p$ and the normalised absorption coefficient $\gamma = \Gamma/\omega_p$ by the formula $\varepsilon_m = 1 - 1/(\tilde{\omega}^2 + i\tilde{\omega}\gamma)$. For silver, $\gamma = 0.01471$.

In the present study we also studied the distribution of the maximum value of the electric field E_a for an oscillation period over spatial points in the plane $\tilde{x}\tilde{z}$. The calculation method consists in the following [20]. First, at the point under study we found complex components $\tilde{E}_{\tilde{x}} = -\partial\tilde{\Phi}/\partial\tilde{x}$ and $\tilde{E}_{\tilde{z}} = -\partial\tilde{\Phi}/\partial\tilde{z}$ of the complex vector of the electric field. Then, we found the real terms of the components $\mathrm{Re}[\tilde{E}_{\tilde{x}}\exp(-i\omega t)]$ and $\mathrm{Re}[\tilde{E}_{\tilde{z}}\exp(-i\omega t)]$ at some point in time t. Finally, we calculated the maximum value of the electric field for the period

$$E_a = \max_{0\leqslant\omega t\leqslant 2\pi}\sqrt{\{\mathrm{Re}[\tilde{E}_{\tilde{x}}\exp(-i\omega t)]\}^2 + \{\mathrm{Re}[\tilde{E}_{\tilde{z}}\exp(-i\omega t)]\}^2}\,.$$

Figures 2a and 2b show the distributions of the electric potential modulus $|\tilde{\Phi}|$ and the maximum field E_a for the silver tip, calculated by the described method, at a frequency $\tilde{\omega} = 0.26053$, corresponding to a wavelength in free space $\lambda = 532$ nm, at which the experiments were carried out in [1]. The tip was located in a medium with $\varepsilon_d = 1$ at a distance $\Delta\tilde{z} = 0.5$ (0.5R) from the half-space filled with a dielectric having $\varepsilon_p = 4$. The distributions have been normalised to unity in the maximum of the field at the top of the tip. The field distribution E_a (Fig. 2b) in the tip apex is shown in more detail in Fig. 2c. For comparison, Fig. 2d shows the distribution $|\tilde{\Phi}|$ for a single tip without a dielectric half-space.

From a comparison of Figs 2a and 2c one can see that the presence of a half-space with a dielectric (boundary $\tilde{z}_0 = 1$) enhances the focusing of the field in the vicinity of the tip apex. Thus, in experiments on scanning of the surface with a surface plasmon wave focused by a nanoapex microtip (to study Raman scattering of molecules at the surface [1]), the presence of a half-space with a dielectric enhances nanofocusing of the electric field in the vicinity of the tip apex and the nearest point on the plane boundary.

Figure 3 shows the same distributions as in Fig. 2, but at a higher frequency ($\tilde{\omega} = 0.62252$). Figure 3a demonstrates the distribution of the electric potential modulus $|\tilde{\Phi}|$ for the silver tip located at the same distance $\Delta\tilde{z} = 0.5$ from a plane boundary of the half-space with $\varepsilon_p = 4$, Fig. 3b – the distribution of the maximum field E_a in the focusing spot, Fig. 3c – a more detailed distribution of E_a (Fig. 3b) in the focal spot, and Fig. 3d – the distribution $|\tilde{\Phi}|$ for a single tip.

One can see from Fig. 3d that for a single tip, the first node of the potential corresponds with great accuracy to the point with the coordinates $\tilde{x} = 1$, $\tilde{z} = 0$; for this purpose we have specially chosen the frequency $\tilde{\omega} = 0.62252$. Figure 3a shows that the first node was shifted closer to the focus, i.e. the focal spot in the presence of a dielectric half-space was smaller, and focusing became sharper. Obviously, this is due to a higher dielectric constant of the half-space ($\varepsilon_p = 4$ vs. $\varepsilon_p = 4$ for a single tip).

Calculations were also performed for a silver tip, located above the half-space filled with silver, in the same geometry at a frequency $\tilde{\omega} = 0.62252$. Figure 4 shows the distribution E_a in the focal spot. One can see that nanofocusing did not disappear in the presence of a metal plane. Thus, investigation of a surface with a surface plasmon wave focused by a microtip nanoapex is applicable for studying both dielectric and metal surfaces.

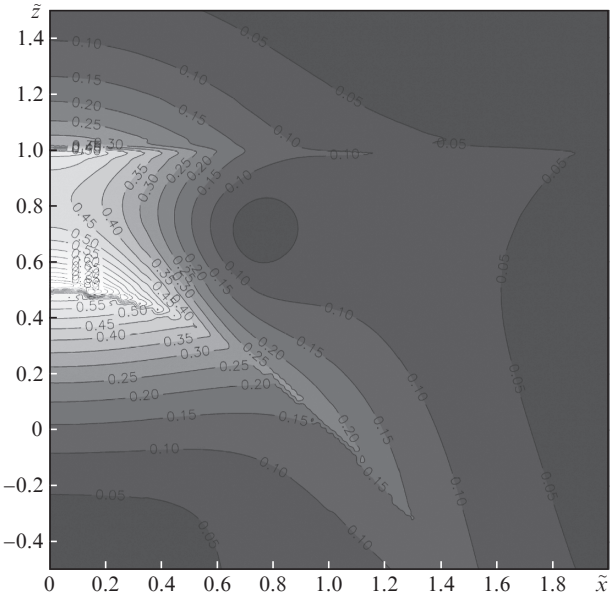

Figure 4. Focal distribution of the maximum field E_a for a silver tip near the flat surface $\tilde{z}_0 = 1$ of the half-space filled with silver, at a frequency $\tilde{\omega} = 0.62252$.

4. Conclusions

We have developed a method for finding the focal distribution of the electromagnetic field near the nanoapex of a metal microtip. The results of calculations show that the presence of

a flat surface of a material near the microtip enhances the focusing. It is found that the presence of a metal surface near the tip does not impair its focusing properties; this allows us to study Raman scattering of molecules located on a flat metal surface in the focusing spot.

Acknowledgements. This work was supported by a grant of the RF Ministry of Education and Science (Research Project 'Creation of electro-optical gradient thin-film structures for precision optics and analytical instrumentation'; Grant Agreement No. 14.579.21.0066 with the RF Ministry of Education and Science dated 10.23.2014, unique identifier RFMEFI 57914 X 0066).

References

1. De Angelis F. et al. *Nat. Nanotechnol.*, **5**, 67 (2010).
2. Frey H.G., Keilmann F., Kriele A., Guckenberger R. *Appl. Phys. Lett.*, **81**, 5030 (2002).
3. Stockman M.I. *Phys. Rev. Lett.*, **93**, 137404 (2004).
4. Petrin A.B. *High Temp.*, **50** (1), 15 (2012).
5. Klimov V., Guzatov D. *Appl. Phys. A*, **89**, 305 (2007).
6. Giugni A., Allione M., Torre B., et al. *J. Opt.*, **16**, 114003 (2014).
7. Giugni A., Torre B., Toma A., et al. *Nat. Nanotechnol.*, **8** (11), 845 (2013).
8. Petrin A.B. *Usp. Prikl. Fiz.*, **3** (3), 236 (2015).
9. Petrin A.B. *Kvantovaya Elektron.*, **45** (7), 658 (2015) [*Quantum Electron.*, **45** (7), 658 (2015)].
10. Klimov V., Guzatov D. *Appl. Phys. A*, **89**, 305 (2007).
11. Klimov V. *Nanoplasmonics* (Singapore: Pan Stanford Publishing, 2014).
12. Klimov V.V. *Nanoplazmonika* (Nanoplasmonics) (Moscow: Fizmatlit, 2010).
13. Passian A., Ritchie R.H., Lereu A.L., Thundat T., Ferrell T.L. *Phys. Rev. B*, **71**, 115425 (2005).
14. Sivukhin D.V. *Obshchii kurs fiziki. T. III. Elektrichestvo* (The General Course of Physics. Vol. III. Electricity) (Moscow: Fizmatlit, 2004).
15. Angot A. *Compléments de mathématiques a l'usage des ingénieurs de l'électrotechnique et des télécommunications* (Paris: Masson, 1961; Moscow: Nauka, 1967).
16. Nikiforov A.F., Uvarov V.B. *Spetsial'nye funktsii matematicheskoi fiziki* (Special Functions of Mathematical Physics) (Moscow: Nauka, 1984).
17. *Matematika. Novoe v zarubezhnoi nauke. Vyp. 29. Chislennye metody teorii difraktsii* (Mathematics. New in Foreign Science. Vol. 29. Numerical Methods of The Theory of Diffraction) (Moscow: Mir, 1982).
18. Petrin A.B. *Prikl. Fiz.*, (1), 11 (2016).
19. Fox M. *Optical Properties of Solids* (New York: Oxford University Press, 2003).
20. Petrin A.B. *Kvantovaya Elektron.*, **46** (2), 159 (2016) [*Quantum Electron.*, **46** (2), 159 (2016)].